



## Molecular Crystals and Liquid Crystals

Publication details, including instructions for authors and subscription information:

<http://www.tandfonline.com/loi/gmcl20>

### Synthesis of Poly(methyl methacrylate) Encapsulated $\text{TiO}_2$ Nanocomposite Particles in Supercritical $\text{CO}_2$

Haldorai Yuvaraj<sup>a</sup>, Won Soo Kim<sup>a</sup>, Jong Tae Kim<sup>a</sup>,  
In Pil Kang<sup>b</sup>, Yeong-Soon Gal<sup>c</sup>, Sok Won Kim<sup>d</sup> &  
Kwon Taek Lim<sup>a</sup>

<sup>a</sup> Department of Imaging System Engineering,  
Pukyong National University, Busan, Korea

<sup>b</sup> Division of Mechanical Engineering, Pukyong  
National University, Busan, Korea

<sup>c</sup> Polymer Chemistry Laboratory, College of  
Engineering, Kyungil University, Hayang,  
Gyeongsangbuk-Do, Korea

<sup>d</sup> Department of Physics, University of Ulsan, Ulsan,  
Korea

Version of record first published: 10 Nov 2009

To cite this article: Haldorai Yuvaraj, Won Soo Kim, Jong Tae Kim, In Pil Kang, Yeong-Soon Gal, Sok Won Kim & Kwon Taek Lim (2009): Synthesis of Poly(methyl methacrylate) Encapsulated  $\text{TiO}_2$  Nanocomposite Particles in Supercritical  $\text{CO}_2$ , Molecular Crystals and Liquid Crystals, 514:1, 25/[355]-35/[365]

To link to this article: <http://dx.doi.org/10.1080/15421400903217611>

Full terms and conditions of use: <http://www.tandfonline.com/page/terms-and-conditions>

This article may be used for research, teaching, and private study purposes. Any substantial or systematic reproduction, redistribution, reselling, loan, sub-licensing, systematic supply, or distribution in any form to anyone is expressly forbidden.

The publisher does not give any warranty express or implied or make any representation that the contents will be complete or accurate or up to date. The accuracy of any instructions, formulae, and drug doses should be independently verified with primary sources. The publisher shall not be liable for any loss, actions, claims, proceedings, demand, or costs or damages whatsoever or howsoever caused arising directly or indirectly in connection with or arising out of the use of this material.

## Synthesis of Poly(methyl methacrylate) Encapsulated TiO<sub>2</sub> Nanocomposite Particles in Supercritical CO<sub>2</sub>

Haldorai Yuvaraj<sup>1</sup>, Won Soo Kim<sup>1</sup>, Jong Tae Kim<sup>1</sup>,  
In Pil Kang<sup>2</sup>, Yeong-Soon Gal<sup>3</sup>, Sok Won Kim<sup>4</sup>, and  
Kwon Taek Lim<sup>1</sup>

<sup>1</sup>Department of Imaging System Engineering, Pukyong National University, Busan, Korea

<sup>2</sup>Division of Mechanical Engineering, Pukyong National University, Busan, Korea

<sup>3</sup>Polymer Chemistry Laboratory, College of Engineering, Kyungil University, Hayang, Gyeongsangbuk-Do, Korea

<sup>4</sup>Department of Physics, University of Ulsan, Ulsan, Korea

*Polymer encapsulated inorganic metal oxide nanocomposites composed of poly (methyl methacrylate)/TiO<sub>2</sub> were synthesized by the radical dispersion polymerization of methyl methacrylate in supercritical carbon dioxide. TiO<sub>2</sub> nanoparticles, pretreated with 3-methacryloxypropyltrimethoxysilane were used to produce the nanocomposites. Relatively stable composite latexes were formed in supercritical carbon dioxide at 7.5% w/w TiO<sub>2</sub> with respect to MMA in the presence of poly (dimethylsiloxane-*b*-methacrylic acid) stabilizer, which resulted in dry white powder. With increasing the ratio of TiO<sub>2</sub>/methyl methacrylate, the latexes became unstable and produced more agglomerated products. Transmission electron microscope images revealed that the nanoparticles were encapsulated as small agglomerate in poly(methyl methacrylate) particles. This facile method provides a way to develop solvent free composites with nanostructures. The composite particles were also confirmed by FT-IR spectroscopy, X-ray diffraction and thermogravimetric analysis.*

**Keywords:** MPTMS; polymer encapsulation; supercritical carbon dioxide; surface modification; TiO<sub>2</sub>

This work was supported by the Korea Science and Engineering Foundation (KOSEF) grant funded by the Korea government (MEST) (No. R01-2008-000-21056-0) and the second stage of BK21 Program.

Address correspondence to Prof. Kwon Taek Lim, Division of Image Science and Engineering, Pukyong National University, San 100 Yongdang-dong, Nam-gu, Busan 608-739, Korea. E-mail: ktlim@pknu.ac.kr

## INTRODUCTION

Organic/inorganic nanocomposites have become an effective source of advanced materials as they usually exhibit unique properties that traditional composites and conventional materials do not have [1,2]. They combine the advantages of the inorganic material (rigidity, high thermal stability) and the organic polymer (flexibility, ductility, and processibility) [3,4]. Especially, titanium dioxide is a fascinating semiconductor for wide applications in catalysis, dielectric ceramics, solar cells and optoelectronic devices. It is also viewed as an important inorganic component in nanocomposites for the improvement of mechanical and dielectrical properties [5]. Poly(methyl methacrylate) and titanium dioxide (PMMA/TiO<sub>2</sub>) nanocomposites have received particular attention due to their potential applications in the capacitors and organic thin film transistors (OTFT). The introduction of nanoparticles into a polymer matrix has proved to be an effective method to improve the performance of polymer materials. Several methods have been used to produce polymer/inorganic oxide nanocomposites, such as sol-gel reaction [6], polymerization via melt-processing [7], and intercalative polymerization [8] depending on the nature of nanoparticles and on the synthetic process of the polymeric matrices. Conventionally, polymerization of monomers and formation of inorganic nanoparticles are separately performed, and the polymer and nanoparticles are mechanically mixed to form nanocomposites [9]. However, it is extremely difficult to disperse the nanoparticles homogeneously into the polymer matrix because of the easy agglomeration of nanoparticles and the high viscosity of polymers. In recent years, much attention has been paid to the *in situ* synthesis, particularly polymer encapsulated inorganic oxide nanocomposites due to their potential applications [10–13]. Therefore it is essential to disperse the nanoparticles before polymerization. Prior to the dispersion; the nanoparticles must be modified with organic materials to improve their compatibility and dispersion. Various methodologies have been used to synthesize composite particles. However, processing of polymers generally employs large quantity of organic solvents that are noxious and harmful to the environment. In addition the residual solvents remained in the polymers limited their applications. Thus, the processing with an environmentally benign supercritical carbon dioxide (scCO<sub>2</sub>) offers an attractive alternative to the conventional processing.

scCO<sub>2</sub> technology has been widely applied in material science because of its unique characteristics such as non-toxic, non-flammable, chemically inert, low viscosity, high diffusivity and near

zero surface tension. In addition, CO<sub>2</sub> has a moderate critical temperature and critical pressure. Moreover carbon dioxide offers high mass transport rates and allows *in situ* removal of unreacted monomers and other impurities [14]. Since scCO<sub>2</sub> has a strong solvent power for dissolving many organic compounds and swelling most organic polymers, it has been successfully utilized in the synthesis of organic/inorganic polymer composites [15–18]. Recently we have demonstrated the synthesis of silica nanoparticles embedded polystyrene microspheres by dispersion polymerization in scCO<sub>2</sub> [19].

In this paper, PMMA/TiO<sub>2</sub> nanocomposite particles are synthesized by *in-situ* radical dispersion polymerization of methyl methacrylate (MMA) in the presence of surface functionalized TiO<sub>2</sub> in scCO<sub>2</sub>. The effect of different loading ratio of the TiO<sub>2</sub>/MMA on the polymerizations is also investigated. The resulting nanocomposites are characterized by FT-IR, SEM, TEM, XRD, and TGA.

## EXPERIMENTAL

### Materials

MMA (Aldrich) was purified by passing through a neutral alumina column to remove the inhibitor. Then it was stored over CaH<sub>2</sub> below 0°C and distilled prior to use. 2,2-azobisisobutyronitrile (AIBN) (Aldrich) was purified by recrystallization in methanol. Titanium dioxide nanoparticles with the average particle size 5 nm (anatase, Aldrich), 3-methacryloxypropyltrimethoxysilane (MPTMS, Aldrich) as a silane coupling agent, and research grade CO<sub>2</sub> (Daeyoung Co., 99.99%) were used as received. Toluene (Aldrich) was stored over CaH<sub>2</sub> below 0°C and distilled prior to use. The block copolymer poly(dimethylsiloxane)-*b*-poly(methacrylic acid) ( $M_n = 5000$  g/mol for PDMS and  $M_n = 1000$  g/mol for PMA) was prepared by group transfer polymerization as described elsewhere [20].

### Surface Modification of TiO<sub>2</sub>

The surface modification reaction was carried out according to the procedure given in the literature [21]. After dispersing 10 g of TiO<sub>2</sub> nanoparticles in 200 mL of toluene, an excess amount of MPTMS was added and the resulting solution was stirred for 24 h under argon atmosphere. Modified TiO<sub>2</sub> was isolated by centrifugation and washed repeatedly with toluene. Finally it was dried at 50°C under vacuum for 24 h. MPTMS changes the TiO<sub>2</sub> surface into hydrophobic and provides methacrylate terminal group for polymer grafting.

## Preparation of PMMA/TiO<sub>2</sub> Nanocomposites

The dispersion polymerization of MMA in scCO<sub>2</sub> was carried out in a 4 mL high pressure view cell reactor. In a typical synthesis of nanocomposite particles, 1 g of MMA, 0.075 g MPTMS functionalized TiO<sub>2</sub>, 0.15 g of stabilizer (PDMA-*b*-PMA), 0.02 g of AIBN, and a Teflon-coated stir bar were placed inside the reactor. The stainless steel reactor was pressurized by ISCO syringe pump (Model 260D) containing compressed CO<sub>2</sub> at a pressure of approximately 7 MPa, and then the reactor was heated to 65°C in a water bath. The remaining CO<sub>2</sub> was added into the reactor at 65°C until the desired pressure of 34.5 MPa was reached, and the polymerization was continued for 12 h. After polymerization, the reactor was cooled in an ice water, and the unreacted MMA was extracted with liquid CO<sub>2</sub> at a flow rate of 20 mL/min. The remaining CO<sub>2</sub> was slowly vented at the end of extraction, and the product was collected and weighed.

## Characterization

FT-IR characterizations of pristine TiO<sub>2</sub>, functionalized TiO<sub>2</sub>, and PMMA/TiO<sub>2</sub> nanocomposites were performed using a BOMEM Hartman & Braun spectrometer. Scanning electron microscopy (SEM) observation was performed using Hitachi S-2400 scanning electron microscope was operated at 20 kV. The TEM images of the powder products were obtained from JEOL, JEM-2010 transmission electron microscope. The XRD patterns of the polymer and composites were collected on a powder X-ray diffractometer (Philips, X'Pert-MPD) with Cu K $\alpha$  radiation. Thermal stability was investigated by thermal gravimetric analyzer (Perkin Elmer, TGA-7) under a nitrogen flow (35 mL/min). The heating rate was 10°C/min.

## RESULTS AND DISCUSSION

In order to obtain PMMA/TiO<sub>2</sub> nanocomposites in scCO<sub>2</sub>, it is necessary to disperse TiO<sub>2</sub> nanoparticles prior to the polymerization. In this work, we used commercially available TiO<sub>2</sub> nanoparticles with the average particle size of 5 nm. The as-received TiO<sub>2</sub> particles were not dispersible in CO<sub>2</sub> but could be dispersed after modification with MPTMS. Similarly we have previously demonstrated the improved dispersion of silica nanoparticles in scCO<sub>2</sub> with MPTMS modification, which is due to the favorable interaction between MPTMS molecules and CO<sub>2</sub> [19]. The surface functionalized TiO<sub>2</sub> was characterized by FT-IR (see Fig. 1). The spectrum showed characteristic absorption

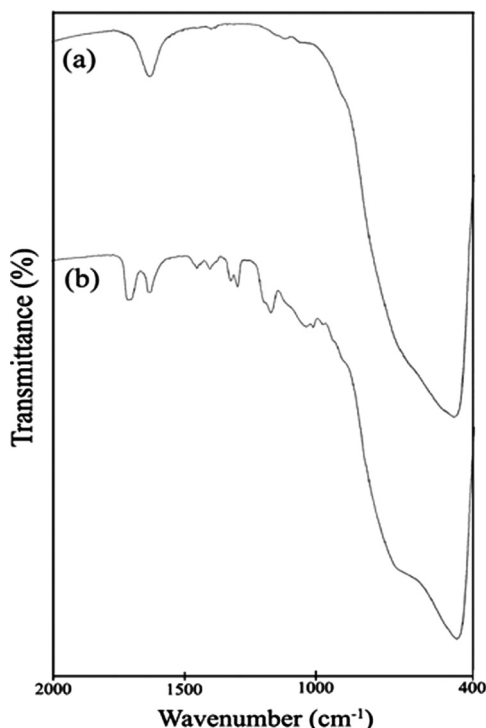


**FIGURE 1** FT-IR spectra of (a) pristine  $\text{TiO}_2$  and (b) surface modified  $\text{TiO}_2$ .

bands:  $\text{CH}_3$  ( $2950\text{--}2920$  and  $1430\text{ cm}^{-1}$ ),  $\text{C}=\text{O}$  ( $\sim 1720\text{ cm}^{-1}$ ),  $\text{C}=\text{C}$  ( $\sim 1635\text{ cm}^{-1}$ ),  $\text{C}-\text{C}$  ( $\sim 1500\text{--}1400\text{ cm}^{-1}$ ) and  $\text{Si}-\text{O}$  ( $\sim 1300\text{--}1250\text{ cm}^{-1}$ ), which indicate the availability of silane group on the surface of the filler [22].

PMMA/ $\text{TiO}_2$  nanocomposites were obtained by the dispersion polymerization of MMA in the presence of surface functionalized  $\text{TiO}_2$  particles dispersed in  $\text{scCO}_2$ . In order to obtain composite particles, it is necessary to disperse the PMMA/ $\text{TiO}_2$  composite latexes in  $\text{scCO}_2$  by using suitable stabilizers. PDMS-*b*-PMA was selected as a stabilizer in this study since it had produced spherical PMMA particles in  $\text{scCO}_2$  [23]. Polymerization reactions were carried out with fixed amount of monomer (25% w/v to  $\text{CO}_2$ ) and stabilizer (15% w/w to monomer), but with varying amount of  $\text{TiO}_2$  nanoparticles (7.5 to 20% w/w to monomer). In all the cases, the particles were initially stable, but they appeared to flocculate and coalesce as the reaction proceeds. At higher concentration of  $\text{TiO}_2$ , the flocculation increased. A free-flowing white powder remained inside the reaction vessel upon

venting the  $\text{CO}_2$  after the completion of polymerization. The successful stabilization of polymerizations using PDMS-*b*-PMA resulted in higher yields. Though the size of particles is similar, it can be seen that the conversion of monomer tends to decrease with increasing the amount of  $\text{TiO}_2$ . Figure 2 shows the representative SEM of the PMMA/ $\text{TiO}_2$  nanocomposites. The composite particles obtained from polymerizations were in the form of spherical with relatively narrow distributions for composites with 7.5%  $\text{TiO}_2$ . Slight aggregation between particles were also observed, which is, however, often seen from the dispersion polymerization with silicone based stabilizers in  $\text{scCO}_2$  [24]. The results clearly indicate that the PDMS-*b*-PMA stabilizer provided an efficient stabilization for the composite latexes to ensure the formation spherical particles. However, the particles become more agglomerated in the case of composites with 15% and 20%  $\text{TiO}_2$ . Several big particles were also found, which is evident from

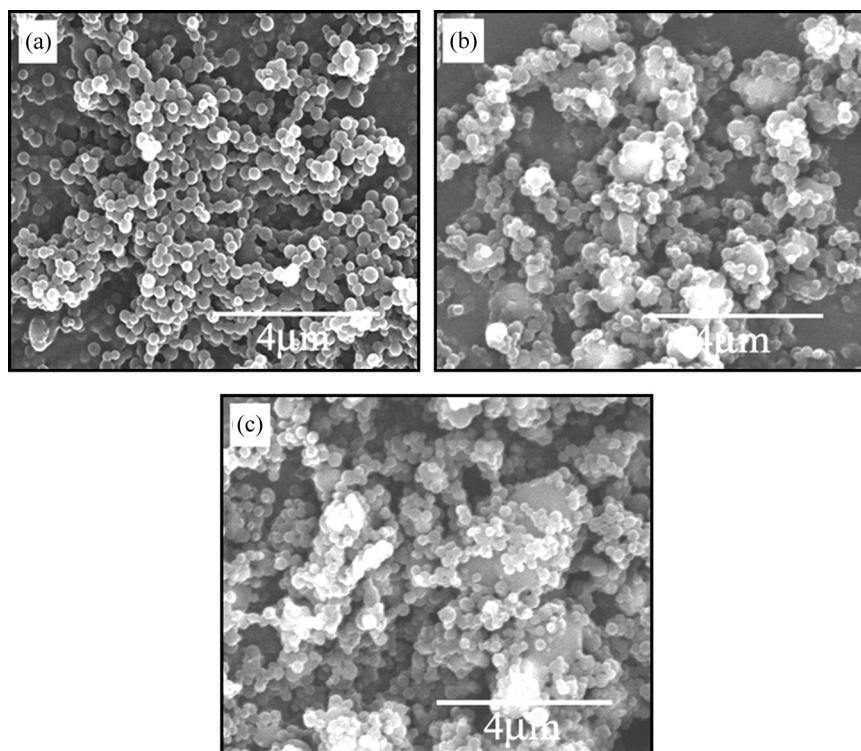
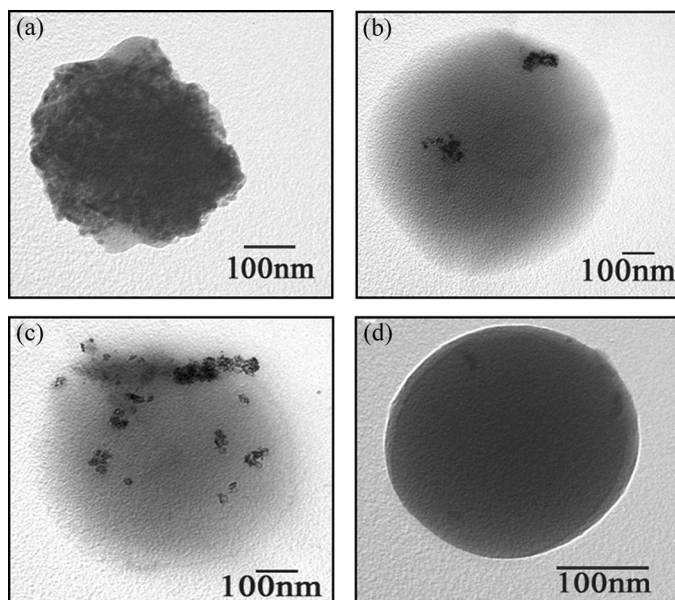


**FIGURE 2** SEM pictures of PMMA/ $\text{TiO}_2$  nanocomposites with (a) 7.5%, (b) 15%, and (c) 20%  $\text{TiO}_2$ .



the SEM images (see Figs. 2(b) and (c)). It is likely that pre-aggregation of nanoparticles was predominant due to the less stabilization of particles in the reaction medium at higher  $\text{TiO}_2$  concentrations. This agglomeration is consistent with visual observation of the flocculation during reaction.

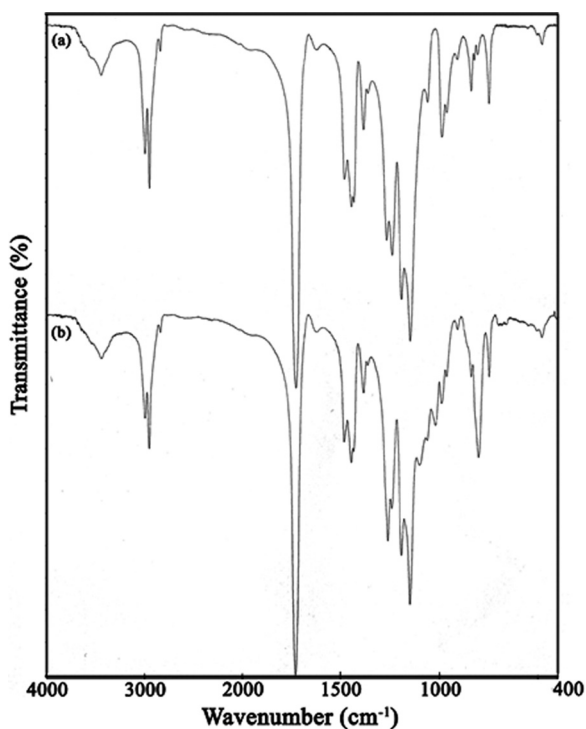
Figure 3 shows the TEM images of PMMA/ $\text{TiO}_2$  nanocomposites, which are clearly evident that the  $\text{TiO}_2$  nanoparticles (dark color) are embedded inside the polymer (light color). But the nanoparticles are not completely embedded inside the polymer as individual particles, whereas several nanoparticles are combined together to form aggregates. This may be due to the fact that the smaller sizes of nanoparticles tend to agglomerate easily. The nature of association between filler and the polymer component showed that almost all  $\text{TiO}_2$  nanoparticles are encapsulated by PMMA, whereas some  $\text{TiO}_2$  particles exist out side of the polymer surface. The  $\text{TiO}_2$  aggregates might not be separated completely into individual particles in the reaction solution prior to polymerization, which is likely the reason for the heterogeneity of morphologies including encapsulated particles, larger aggregates and free PMMA particles. This can be attributed to the fact that, with the increasing amount of  $\text{TiO}_2$  particles in the composites,



**FIGURE 3** TEM images of PMMA/ $\text{TiO}_2$  nanocomposites.

the percentage of grafting onto the polymer decreases. From the TEM as well SEM micrographs, it is clear that the particle agglomeration is directly proportional to the amount of  $\text{TiO}_2$  loaded.

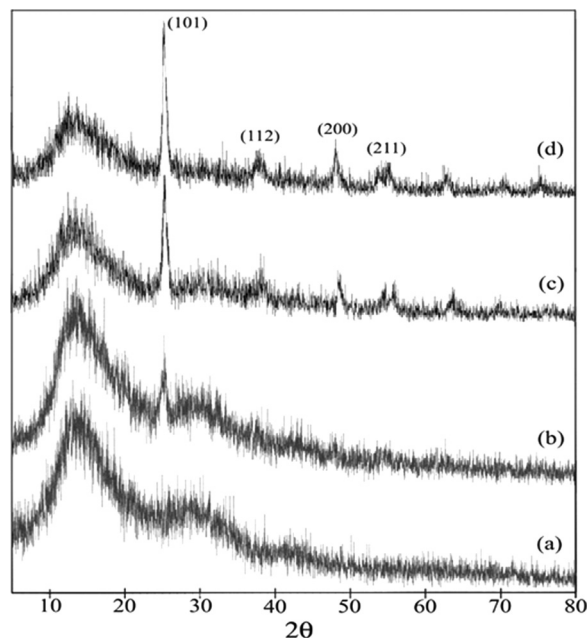
Figure 4 shows the FTIR spectra of the PMMA and nanocomposites. The assignments of the stretching vibration bands of the C=O and C-H bonds in the PMMA segment are at  $1730$  and  $2953\text{ cm}^{-1}$ , respectively. Stretching vibration bands of C-O-C or Si-O-Si and Si-C bonds are observed at  $1023$ – $1194$  and  $1263\text{ cm}^{-1}$ , respectively. The peak centered at  $625\text{ cm}^{-1}$  is accounted for the vibrations of Ti-O-Ti groups and is regarded as the characteristic peak for  $\text{TiO}_2$ . The Ti-OH band in the spectra of PMMA/ $\text{TiO}_2$  is observed as a broad absorption in the range of  $3400$ – $3500\text{ cm}^{-1}$ . The position of the Ti-OH absorption band is below  $3500\text{ cm}^{-1}$ . This is probably because of the hydrogen bonding of the Ti-OH residue group with the carbonyl group. The positions of the above absorption bands are similar to those reported in the literature [25].



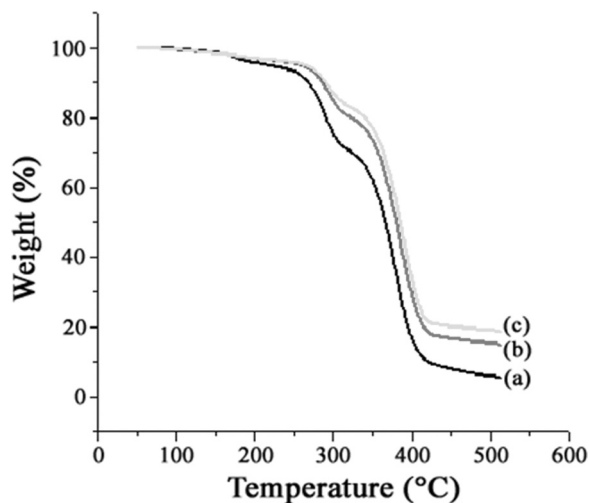
**FIGURE 4** FT-IR spectra of (a) PMMA and (b) the nanocomposite.

Figure 5 shows the XRD curves of PMMA, PMMA/TiO<sub>2</sub> nanocomposites. It is clear that the PMMA prepared in the absence of TiO<sub>2</sub> nanoparticles is amorphous. The nanocomposites with 7.5% TiO<sub>2</sub> exhibits weak peaks at  $2\theta = 55.08^\circ$  and  $25.35^\circ$  are corresponding to (211) and (101) crystal planes of the anatase TiO<sub>2</sub>. The low intensities of these peaks indicate that the nanocomposite is still largely amorphous. By contrast, the composites with 15% TiO<sub>2</sub> demonstrated enhanced crystallization, which is represented by slight higher peak intensity of the same crystal planes, and the appearance of additional diffraction peaks at  $2\theta = 38.63^\circ$  and  $48.12^\circ$ , corresponding to (112) and (200) crystal planes. A further increase in the intensity of these peaks is demonstrated by the nanocomposites with 20% TiO<sub>2</sub>.

Figure 6 illustrates the TGA curves of PMMA/TiO<sub>2</sub> nanocomposites at a heating rate of 10°C/min under nitrogen atmosphere. It is known that radically polymerized PMMA starts to degrade by initiation at the head-to-head linkages (at around 160°C), initiation at the unsaturated ends (at around 270°C), and random initiation along the polymer back bone (at around 360°C) [26]. The as prepared PMMA/TiO<sub>2</sub>



**FIGURE 5** XRD patterns of (a) PMMA, PMMA/TiO<sub>2</sub> nanocomposites with, (b) 7.5%, (c) 15%, and (d) 20% TiO<sub>2</sub>.



**FIGURE 6** TGA curves of PMMA/TiO<sub>2</sub> nanocomposites with (a) 7.5% (b) 15% and (c) 20% TiO<sub>2</sub>.

nanocomposites have thermal decomposition temperatures of 285–420°C. These values are ascribed that the decomposition temperature of PMMA segment. Notably the decomposition temperature for the composites are shifted to a higher temperature range as the ratio of TiO<sub>2</sub>/PMMA increases, which indicates the enhancement of thermal stability of the composites. As expected, the residue amount of composites at 600°C increased with increasing TiO<sub>2</sub> content in the composite material.

## CONCLUSION

PMMA/TiO<sub>2</sub> nanocomposite particles were synthesized via dispersion polymerization in supercritical CO<sub>2</sub> with the aid of the stabilizer PDMS-*b*-PMA. TiO<sub>2</sub> nanoparticles were first surface grafted by coupling agent MPTMS, possessing methacrylate end group which copolymerize with MMA. The MPTMS modified nanoparticles were well dispersed in CO<sub>2</sub>/MMA reaction solution to form stable composite latexes by the dispersion polymerization of MMA. The TEM photographs showed that TiO<sub>2</sub> nanoparticles were encapsulated by the polymer. The SEM images indicated that the composite particles were spherical in morphology. At 7.5% w/w TiO<sub>2</sub> with respect to MMA, dry white uniform spherical particles were produced, while much agglomerated particles were resulted from 15% w/w TiO<sub>2</sub> due to the

insufficient stabilization of latexes in CO<sub>2</sub>. The thermal stabilities of nanocomposites are higher than the bare polymer. This type of solvent free nanocomposites can be applied to an embedded capacitor or an insulating layer for organic thin film transistor.

## REFERENCES

- [1] Mukheerjee, M., Datta, A., & Chakravorty, D. (1994). *Appl. Phys. Lett.*, *64*, 1159.
- [2] Chen, T. K., Tien, Y. L., & Wei, K. H. (2000). *Polymer*, *41*, 1345.
- [3] Okamoto, M., Morita, S., Taguchi, H., Kim, Y. H., Kotaka, S., & Tateyama, H. (2000). *Polymer*, *41*, 3887.
- [4] Avella, M., Errico, M. E., & Martuscelli, E. (2001). *Nano. Lett.*, *4*, 213.
- [5] Thompson, L. & Yates, J. T. (2006). *Chem. Rev.*, *106*, 4428.
- [6] Noell, J. L. W., Wilders, G. L., & McGrath, J. E. J. (1990). *Appl. Polym. Sci.*, *40*, 1177.
- [7] Vaia, R. A., Jandt, K. D., & Giannelis, E. P. (1990). *Macromolecules*, *28*, 8080.
- [8] LeBaron, P. C. & Wang, Z. (1999). *J. Appl. Clay. Sci.*, *15*, 11.
- [9] Ghosh, K. & Maiti, S. N. (1996). *J. Appl. Polym. Sci.*, *60*, 323.
- [10] Caruso, F., Caruso, R. A., & Mohwald, H. (1998). *Science*, *282*, 1111.
- [11] Davies, R., Schurr, G. A., Meenan, P., Nelson, R. D., Bergna, H. E., Brevet, C. A. S., & Goldbaum, R. H. (1998). *Adv. Mater.*, *10*, 1264.
- [12] Oldfield, G., Ung, T., & Mulvaney, P. (2000). *Adv. Mater.*, *12*, 1519.
- [13] Zhang, K., Chen, H., Chen, X., Chen, Z., Cui, Z., & Yang, B. (2003). *Macromol. Mater. Eng.*, *288*, 380.
- [14] Jessop, P. G., *et al.* (1999). *Chemical Synthesis Using Supercritical Fluids*, Wiley-VCH: Weinheim.
- [15] Yuvaraj, H., Woo, M. H., Park, E. J., Jeong, Y. T., & Lim, K. T. (2008). *Eur. Polym. J.*, *44*, 637.
- [16] Yuvaraj, H., Park, E. J., Gal, Y.-S., & Lim, K. T. (2008). *Colloids and Surfaces A: Physicochem. Eng. Aspects*, *313–314*, 300.
- [17] Wang, W., Howdle, S. M., & Yan, D. (2005). *Chem. Commun.*, *31*, 3939.
- [18] Charpentier, P. A., Xu, W. Z., & Li, X. (2007). *Green Chem.*, *9*, 768.
- [19] Do, K. M., Yuvaraj, H., Woo, M. H., Kim, H. G., Jeong, E. D., Johnston, K. P., & Lim, K. T. (2008). *Colloid. Polym. Sci.*, *286*, 1343.
- [20] Lim, K. T., Webber, S. E., & Johnston, K. P. (1999). *Macromolecules*, *32*, 2811.
- [21] Tsubokawa, N., Maruyama, K., Sone, Y., & Shimomura, M. (1989). *Polym. J.*, *21*, 475.
- [22] Domingo, C., Loste, E., & Fraile, J. J. (2006). *Supercrit. Fluids*, *37*, 72.
- [23] Ganapathy, H. S., Hwang, H. S., Jeong, Y. T., & Lim, K. T. (2006). *Stud. Surf. Sci. Catal.*, *159*, 797.
- [24] Yates, M. Z., Li, G., Shim, J. J., Maniar, S., Johnston, K. P., Lim, K. T., & Webber, S. E. (1999). *Macromolecules*, *32*, 1018.
- [25] Chen, W. H., Lee, S. J., Lee, L. H., & Lin, J. L. (1999). *J. Mater. Chem.*, *9*, 2999.
- [26] Kashiwagi, T., Inaba, A., Brown, J. E., Hatada, K., Kitayama, T., & Masuda, E. (1986). *Macromolecules*, *19*, 2160.